



# $\gamma\delta$ T cells in human colon adenocarcinomas comprise mainly V $\delta$ 1, V $\delta$ 2, and V $\delta$ 3 cells with distinct phenotype and function

William Rodin<sup>1</sup> · Louis Szeponik<sup>1</sup> · Tsvetanka Rangelova<sup>1</sup> · Firaol Tamiru Kebede<sup>2</sup> · Tobias Österlund<sup>3,4</sup> · Patrik Sundström<sup>1</sup> · Stephen Hogg<sup>1</sup> · Yvonne Wettergren<sup>5,6</sup> · Antonio Cosma<sup>7</sup> · Anders Ståhlberg<sup>2,3,4</sup> · Elinor Bexé Lindskog<sup>5,6</sup> · Marianne Quiding Järbrink<sup>1</sup>

Received: 16 January 2024 / Accepted: 11 June 2024 / Published online: 2 July 2024  
© The Author(s) 2024

## Abstract

$\Gamma\delta$  T cell infiltration into tumours usually correlates with improved patient outcome, but both tumour-promoting and tumoricidal effects of  $\gamma\delta$  T cells have been documented. Human  $\gamma\delta$  T cells can be divided into functionally distinct subsets based on T cell receptor (TCR) V $\delta$  usage. Still, the contribution of these different subsets to tumour immunity remains elusive. Here, we provide a detailed  $\gamma\delta$  T cell profiling in colon tumours, using mass and flow cytometry, mRNA quantification, and TCR sequencing.  $\delta$  chain usage in both the macroscopically unaffected colon mucosa and tumours varied considerably between patients, with substantial fractions of V $\delta$ 1, V $\delta$ 2, and non-V $\delta$ 1 V $\delta$ 2 cells. Sequencing of the V $\delta$  complementarity-determining region 3 showed that almost all non-V $\delta$ 1 V $\delta$ 2 cells used V $\delta$ 3 and that tumour-infiltrating  $\gamma\delta$  clonotypes were unique for every patient. Non-V $\delta$ 1 V $\delta$ 2 cells from colon tumours expressed several activation markers but few NK cell receptors and exhaustion markers. In addition, mRNA analyses showed that non-V $\delta$ 1 V $\delta$ 2 cells expressed several genes for proteins with tumour-promoting functions, such as neutrophil-recruiting chemokines, Galectin 3, and transforming growth factor-beta induced. In summary, our results show a large variation in  $\gamma\delta$  T cell subsets between individual tumours, and that V $\delta$ 3 cells make up a substantial proportion of  $\gamma\delta$  T cells in colon tumours. We suggest that individual  $\gamma\delta$  T cell composition in colon tumours may contribute to the balance between favourable and adverse immune responses, and thereby also patient outcome.

**Keywords**  $\gamma\delta$  T cells · Colon cancer · Tumour immunity · TCR $\delta$  chain

✉ Marianne Quiding Järbrink  
marianne.quiding@microbio.gu.se

- 1 Department of Immunology and Microbiology, Institute of Biomedicine, University of Gothenburg, Sahlgrenska Academy, Gothenburg, Sweden
- 2 Department of Laboratory Medicine, Sahlgrenska Center for Cancer Research, Institute of Biomedicine, University of Gothenburg, Sahlgrenska Academy, Gothenburg, Sweden
- 3 Wallenberg Centre for Molecular and Translational Medicine, University of Gothenburg, Gothenburg, Sweden
- 4 Department of Clinical Genetics and Genomics, Sahlgrenska University Hospital, Gothenburg, Sweden
- 5 Department of Surgery, Institute of Clinical Sciences, University of Gothenburg, Sahlgrenska Academy, Gothenburg, Sweden
- 6 Department of Surgery, Region Västra Götaland, Sahlgrenska University Hospital, Gothenburg, Sweden
- 7 National Cytometry Platform, Luxembourg Institute of Health, Esch-sur-Alzette, Luxembourg

## Abbreviations

CDR3	Complementarity-determining region 3
CRC	Colorectal cancer
MSI	Microsatellite instable
MSS	Microsatellite stable
PBMC	Peripheral blood mononuclear cells
PMA	Phorbol 12-myristate 13-acetate
TCR	T cell receptor
TGFBI	Transforming growth factor-beta induced

## Background

$\Gamma\delta$  T cells are unconventional T cells expressing a semi-variable T cell receptor (TCR) composed of a limited selection of  $\gamma$  and  $\delta$  chains, which bind to invariant MHC I-like molecules, as well as other stress-induced cell surface proteins. Cognate TCR binding leads to immediate effector functions, such as cytotoxicity and cytokine secretion. Human  $\gamma\delta$  T cells are usually characterized based on  $\delta$  chain

usage, where V $\delta$ 1, V $\delta$ 2, and V $\delta$ 3 are the most common. Furthermore, the preferential pairing of different  $\delta$  and  $\gamma$  chains divide  $\gamma\delta$  T cells into additional subsets [1, 2]. Oligoclonal populations of  $\gamma\delta$  T cells are present in different tissues, such as mucosal tissues, skin, and peripheral blood [3]. In humans, V $\delta$ 2 cells dominate in the circulation, while V $\delta$ 1 cells are more common in the intestinal mucosa [1–3]. In addition to the TCR, both V $\delta$ 1 and V $\delta$ 2 cells express various NK cell receptors that react to the expression of surface molecules induced in both infected and transformed cells. Especially the expression of NKp30 and NKp46 has been shown to delineate subsets of  $\gamma\delta$  T cells with increased cytotoxic capacity towards tumour cells [4, 5]. When activated,  $\gamma\delta$  T cells also produce pro-inflammatory cytokines in addition to their cytotoxic functions [6]. In a cancer setting, the infiltration of  $\gamma\delta$  T cells has been associated with an improved clinical outcome in studies across several types of haematological malignancies and solid tumours, including colorectal cancer (CRC) [7–9]. However, in studies with a CRC focus,  $\gamma\delta$  T cells were both positively and negatively correlated to a favourable patient outcome [8, 10, 11]. Generally, anti-tumour immunity and a beneficial patient response are commonly associated with cytotoxicity and the production of Th1 type cytokines [12–14]. As conventional T cells,  $\gamma\delta$  T cells can be divided into different subsets based on cytokine production. In tumour immunity, the two best described are  $\gamma\delta$ 1 and  $\gamma\delta$ 17 cells, with a cytokine profile similar to Th1 and Th17 cells, respectively, and the proportions of these cells detected in different studies vary considerably [15, 16].

There is currently a lack of understanding of which  $\gamma\delta$  T cell subsets contribute to a pro- or anti-tumour immune response, and how they distribute in individual tumours. In this study, we could show that  $\gamma\delta$  T cells-infiltrating colon tumours express V $\delta$ 1, V $\delta$ 2, or V $\delta$ 3 TCR $\delta$  chains and that these subsets are distinct from circulating  $\gamma\delta$  T cells. The proportions of these cells varied considerably among tumours, as did the clonotypes detected, which were all private to a single tumour. We identified a substantial presence of V $\delta$ 3 cells in colon tumours which had reduced anti-tumour effector functions and expressed several tumour-promoting mediators.

## Material and methods

### Patient samples

This study was performed at the Sahlgrenska Academy at the University of Gothenburg together with the Sahlgrenska University Hospital. All procedures and experiments were performed in accordance with the Declaration of Helsinki and were approved by the Regional Research Ethics Committee of western Sweden (reference no 249–15). Venous

blood, macroscopically unaffected colon mucosa (collected at least 10 cm away from the tumour border), and tumour tissue were collected from 45 colon cancer patients (25 males and 20 females, aged 38 to 90, median age 75) undergoing resection surgery for stage I–IV tumours. Cells from 15 of these patients were used for mass cytometry, 27 for flow cytometry analyses, and 3 for both mass and flow cytometry. See Suppl. Table S1 for additional patient and tumour characteristics. In a separate set of 10 patients, comprising 7 males and 3 females, aged 51–89 (Suppl. Table S1), we analysed the TCR repertoire in resected tumour tissues. None of the patients had undergone radio- or chemotherapy during the last 2 years. Microsatellite status was determined as previously described using the microsatellite instability (MSI) Analysis System v.1.2 (ProMega) [17]. MSI-High (MSI-H) tumours were defined as tumours with more than 1 marker showing instability, MSI-Low (MSI-L) as tumours with one marker showing instability, and microsatellite stable (MSS) tumours as tumours with no markers showing instability.

### Cell isolation and stimulation

The tissue material was collected during surgery and transported in ice-cold PBS before isolation of lymphocytes within two hours, and lamina propria lymphocytes were isolated as previously described [18]. Venous blood samples were collected in heparinized tubes during surgery, and peripheral blood mononuclear cells (PBMCs) were isolated by density-gradient centrifugation using Ficoll-Paque (GE Healthcare Bio-Sciences AB).

Enrichment of CD45<sup>+</sup> cells was performed before mass cytometry using the REAlease TIL MicroBead kit (Miltenyi). Cells were kept overnight at 37 °C for functional assays and mass cytometry analysis or at 4 °C for phenotypic analysis using flow cytometry. For cytokine production analyses, cells were incubated overnight in culture medium at 37 °C before polyclonal stimulation the following morning using 50 ng/mL of phorbol 12-myristate 13-acetate (PMA) and 680 ng/mL of ionomycin calcium salt (Sigma-Aldrich) for 4 h, together with a protein transport inhibitor (BD Golgi stop, BD Biosciences).

### $\gamma\delta$ TCR sequencing

Resected tissue samples were cut into smaller pieces and immediately frozen and stored in liquid nitrogen in advanced DMEM/F12 (Thermo Fisher) substituted with 100 U/ml of Penicillin and 100  $\mu$ g/ml of Streptomycin, 10 mM HEPES, Glutamax according to the supplier's recommendation (Gibco), and 10% dimethylsulphoxid (DMSO) until isolation of lymphocytes as previously described [19].  $\gamma\delta$  TCR sequencing was performed on DNA extracted from the isolated lymphocytes with the QIAamp Blood Mini

Kit (Qiagen), according to the manufacturer's instructions. A total of 1.5 µg DNA was analysed using SiMSen-Seq [20], except for one patient (Patient#405) where only 1 µg DNA was available. Library quantity and size distribution were assessed on a Fragment Analyzer using HS NGS Fragment kit (Agilent Technologies). The libraries were pooled at equimolar concentration and purified with a Pip-pinn Prepp using 2% agarose gel reagent kit (Sage Science). Final libraries were quantified with quantitative PCR and then sequenced on the MiniSeq Sequencing System using paired-end and 2 times 150 bp sequencing (Illumina). The raw sequencing data in fastq format have been deposited to the NCBI short read archive (SRA; <https://www.ncbi.nlm.nih.gov/sra>) with accession number PRJNA1107040.

The raw sequencing reads for  $\gamma\delta$  TCR sequencing were analysed with the MIGEC bioinformatics pipeline [21], including unique molecular identifier extraction, consensus read assembly, and annotation of the complementarity-determining region 3 (CDR3) region including annotation of V, D, and J segments, by blasting to known CDR3 sequences.

### Mass cytometry

Mass cytometry analysis was performed as previously described [22], using live cell barcoding with CD45 antibodies conjugated to different isotopes to individually label cells from blood, unaffected colon mucosa, and tumour samples [23]. For a detailed antibody list, see Suppl. Table S2.

### Flow cytometry

Single cell suspensions were stained with a live/dead exclusion dye followed by antibodies to surface antigens. For detection of cytokines and GrB, cells were fixed and permeabilised using the FoxP3 staining kit (eBioscience). For a detailed antibody list, see Suppl. Table S3. The samples were acquired on a BD LSR Fortessa. Samples with fewer than 50 cells of any of the investigated subsets (V $\delta$ 1, V $\delta$ 2, and non-V $\delta$ 1V $\delta$ 2 cells) were not included in the phenotypic or functional analyses.

### mRNA quantification

Live V $\delta$ 1, V $\delta$ 2, and non-V $\delta$ 1V $\delta$ 2 cells from 4 colon tumours were sorted using a BD FACS-Aria Fusion. Multiplex mRNA quantification was performed using the nCounter Analysis system together with the nCounter human Immunology v2 panel (Nanostring) at KIGene (Karolinska Institutet, Stockholm). Nanostring data were normalized to adjust for platform-associated and sample input variations and thresholds were set according to Nanostring guidelines (0, 3–3 for the positive control normalization and 0, 1–10 for the housekeeping gene normalization). The V $\delta$ 1 cells from

one patient were subsequently excluded from analysis due to low RNA quality. The normalized data have been deposited to Gene Expression Omnibus (GEO; <https://www.ncbi.nlm.nih.gov/geo/>) with accession number GSE266504.

### Immunofluorescence

Four-µm cuts from formalin-fixed paraffin-embedded tissue blocks of unaffected mucosa and colorectal tumours were mounted on Superfrost Plus microscope slides. Sections were deparaffinized and rehydrated, and antigens were unmasked with pH9 Tris–EDTA buffer. Tissue was stained with CD3 (A0452, Agilent; Opal 570), CD8 $\alpha$  (SP16, Thermo Fisher Scientific; Opal 620), TCR $\delta$  (H41, Santa Cruz Biotechnologies; Opal 690), pan-cytokeratin (KRT/1877R, Abcam; Opal 520), respectively, using the Opal Polaris 7-Color Manual IHC Kit (Akoya Biosciences). Subsequently, nuclei were stained with spectral DAPI (Akoya Biosciences) and slides were mounted with ProLong Glass Antifade Mounting media (Thermo Fisher Scientific). Tissue sections were scanned with the Metafer Slide Scanning Platform (Axio Imager.Z2 Microscope and 20x/0.8/air objective, Zeiss) equipped with a SpectraSplit filter system (Kromnigon). Images were analysed with Strataquest (TissueGnostics).

### Data processing and statistical analysis

Mass cytometry data were analysed using OMIQ version 10. All clusters that contributed with less than 1% of all  $\gamma\delta$  T cells were excluded from the analysis. Data from the multiplex mRNA quantification were analysed using the Nsolver software (version 4). Flow cytometry data were analysed using FlowJo version 10 and OMIQ version 10. Gini-Simpson diversity index was calculated using the Diverse package in R (version 0.1.5). Statistical analyses of paired data were performed using two-tailed Wilcoxon matched-pairs signed rank test and of unpaired data using two-tailed Mann–Whitney test. When comparing three groups of matched data, the Friedman test followed by Dunn's post-test was used to achieve multiplicity adjusted P values. Statistical tests were performed using GraphPad PRISM version 9. *P*-values < 0.05 were considered statistically significant.

## Results

### $\gamma\delta$ T cells in colon tumours

To investigate the subsets of  $\gamma\delta$  T cells present in colon tumours, we used fresh samples recovered from patients undergoing resection surgery. Using flow cytometry,  $\gamma\delta$  T cells were identified as CD3<sup>+</sup> cells stained by a pan- $\gamma\delta$ -TCR

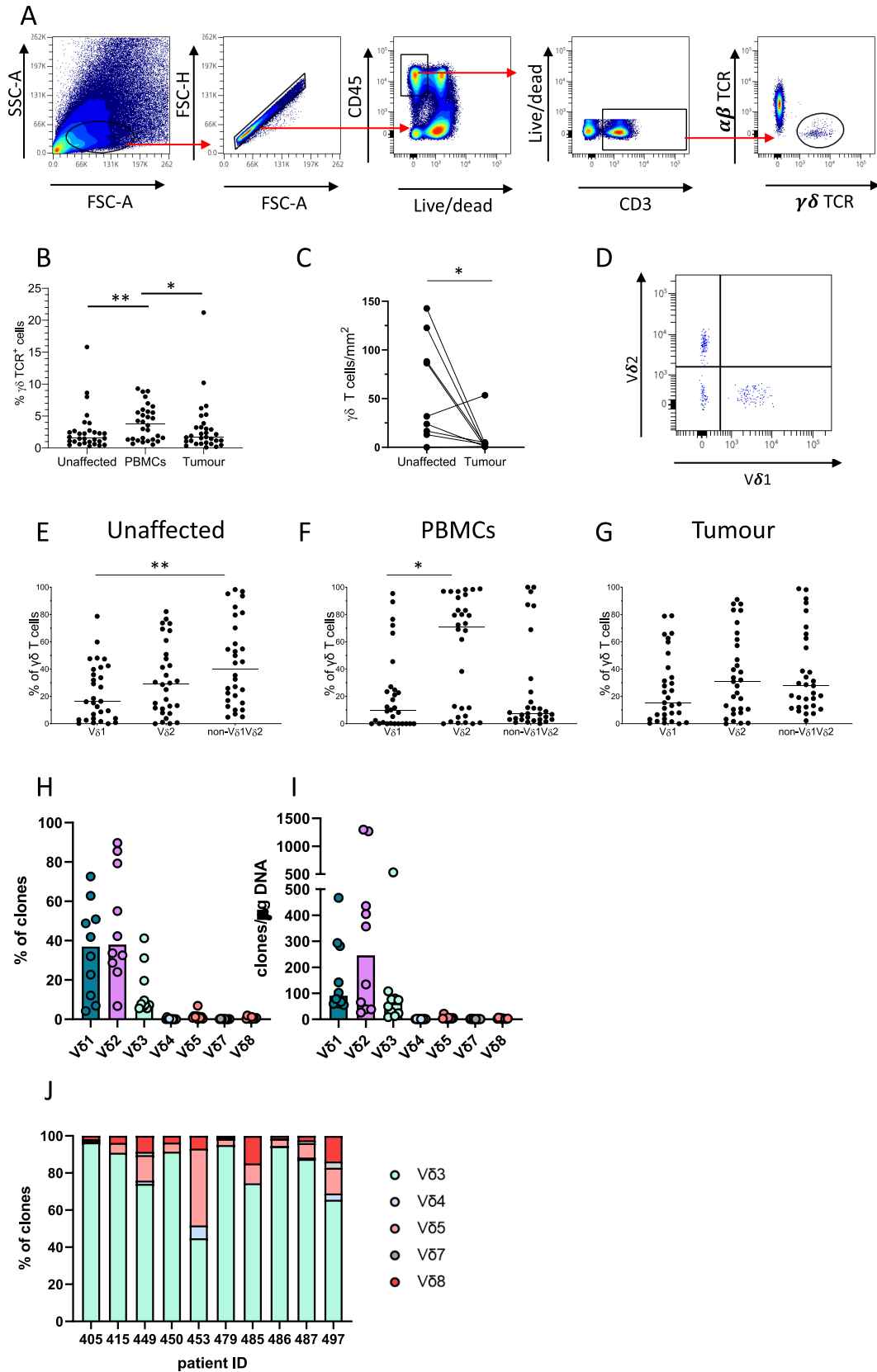


**Fig. 1** Identification of tumour-infiltrating  $\gamma\delta$  T cells. Single cell suspensions were isolated from tumours, corresponding unaffected colon mucosa, and blood, and the frequencies of  $\gamma\delta$  T cells among the CD3<sup>+</sup> T cells were analysed using flow cytometry, immunofluorescence, and CDR3 sequencing. **A** Gating strategy from a representative tumour sample. **B** Frequencies of  $\gamma\delta$  T cells among all CD3<sup>+</sup> lymphocytes determined by flow cytometry. **C** Density of  $\gamma\delta$  T cells determined by fluorescence microscopy in sections from formalin-fixed tumours and corresponding unaffected colon mucosa. **D** Flow cytometry staining of V $\delta$ 1 and V $\delta$ 2 in a representative tumour sample of  $\gamma\delta$  T cells gated as in (a). **E–G** Usage of the V $\delta$ 1 and V $\delta$ 2 chains by  $\gamma\delta$  T cells was determined by flow cytometry in cell suspensions from unaffected colon mucosa (**E**), blood (**F**), and tumour (**G**). **H** V $\delta$  chain usage was determined by CDR3 sequencing in  $\gamma\delta$  T cells isolated from colon tumours and the percentage of clones using the respective V $\delta$  segments or (**I**) the number of clones using each V $\delta$  segment per  $\mu\text{g}$  of DNA is shown for each patient. In (**I**) values less than 1 were set at 1 to improve visualization. **J** Distribution of non-V $\delta$ 1V $\delta$ 2 clones in the individual tumours. Symbols represent individual values and lines the median. In (**C**), symbols are connected to show corresponding values from the same patients. Data in (**B**), (**E**), (**F**), and (**G**) were analysed using two-tailed Friedman test followed Dunn's post-test and in (**C**) using two-tailed Wilcoxon test. \* $p < 0.05$  and \*\* $< 0.01$ .  $n = 10$  for immunofluorescence and CDR3 sequencing, and  $n = 30$  for flow cytometry analyses

antibody but not by a pan- $\alpha\beta$ -TCR antibody (Fig. 1A).  $\gamma\delta$  T cell frequencies were significantly lower in both the tumours and the macroscopically unaffected colon compared to in the blood (Fig. 1B). Using fluorescence microscopy, we also analysed the numbers of  $\gamma\delta$  T cells present in the tumours and unaffected colon mucosa. Here, the numbers of  $\gamma\delta$  T cells were also significantly reduced ( $p < 0.05$ ) in the tumour compared to the unaffected colon mucosa from the same individuals (Fig. 1C, Suppl. Fig. S1). These analyses also showed that  $\gamma\delta$  T cells in the tumours were primarily positioned in the stroma rather than in the tumour epithelium.

To further define the TCRs of tumour-infiltrating  $\gamma\delta$  T cells, we analysed the V $\delta$  chain usage (Fig. 1D). The dominating subset in the circulation was V $\delta$ 2 cells. In the tissue, there were also considerable numbers of V $\delta$ 2 cells in both unaffected mucosa and tumours, while V $\delta$ 1 cells were less numerous in most patients. We could also document a substantial proportion of  $\gamma\delta$  T cells that did neither express V $\delta$ 1 nor V $\delta$ 2. These non-V $\delta$ 1V $\delta$ 2 cells were present in both tumour and unaffected mucosa from all patients (Fig. 1E–G). Quantitative V $\delta$  CDR3 sequencing analyses clearly showed that the large majority of non-V $\delta$ 1 V $\delta$ 2 cells in the tumours used V $\delta$ 3. Only one out of ten patients displayed a sizeable V $\delta$ 5 population alongside the V $\delta$ 3 cells (Fig. 1H, I, J).

V $\delta$ 2 cells are divided into two main types based on their usage of the V $\gamma$ 9 chain. The classical, innate-like V $\gamma$ 9<sup>+</sup>V $\delta$ 2<sup>+</sup> cells are the most common, while the rarer V $\gamma$ 9<sup>-</sup>V $\delta$ 2<sup>+</sup> cells have been described as a more adaptive-like cell type with a more diverse TCR [24].  $\gamma\delta$  T cells expressing the V $\gamma$ 9 chain were common in all tissues, and V $\gamma$ 9 was most commonly paired with V $\delta$ 2 (Fig. 2A). However, we also found

fractions of both V $\delta$ 1 and non-V $\delta$ 1V $\delta$ 2 cells in all tissues that expressed the V $\gamma$ 9 chain (Suppl. Fig. S2). V $\gamma$ 9<sup>-</sup>V $\delta$ 2<sup>+</sup> cells were present to some extent in tissue samples and blood from most patients (Fig. 2B). We also detected low to moderate expression of CD8 in all subsets of  $\gamma\delta$  T cells investigated in all the tissues examined (Suppl Fig. S3).

Different naïve and memory populations of  $\gamma\delta$  T cells can be distinguished based on the expression of CD45RA and CD27, defining naïve (CD45RA<sup>+</sup>CD27<sup>+</sup>), central memory (T<sub>CM</sub>, CD45RA<sup>-</sup>CD27<sup>+</sup>), effector memory (T<sub>EM</sub>, CD45RA<sup>-</sup>CD27<sup>-</sup>), and terminally differentiated effector memory (T<sub>EMRA</sub>, CD45RA<sup>+</sup>CD27<sup>-</sup>) cells [25]. This classification was originally devised for conventional  $\alpha\beta$  T cells and may not be directly applicable to  $\gamma\delta$  T cells, but we have used it here for convenience. The V $\delta$ 1 cells in the tumours and unaffected mucosa were usually dominated by T<sub>EM</sub> cells, while circulating V $\delta$ 1 cells were dominated by naïve and T<sub>EMRA</sub> cells (Fig. 2C). V $\delta$ 2 cells were similar to each other in all the examined locations and dominated by cells with a T<sub>CM</sub> phenotype (Fig. 2D). In the non-V $\delta$ 1V $\delta$ 2 cells in the colon mucosa and the tumours, the naïve cells were more prominent than in V $\delta$ 1 and V $\delta$ 2, and there was also a strong component of T<sub>EM</sub> cells in the non-V $\delta$ 1V $\delta$ 2 subset. In addition, the circulating non-V $\delta$ 1V $\delta$ 2 cells were dominated by T<sub>EMRA</sub> cells (Fig. 2E).

Taken together, these results show that  $\gamma\delta$  T cells do not infiltrate colon tumours to the same extent as the surrounding unaffected colon mucosa, but that there is a prominent subset of non-V $\delta$ 1V $\delta$ 2 cells primarily made up of V $\delta$ 3 cells in the tumours.

### Infiltration of non-V $\delta$ 1V $\delta$ 2 cells in relation to clinicopathologic features

As the size of the non-V $\delta$ 1V $\delta$ 2 subset varied considerably between patients, we were interested to relate their presence to clinicopathologic features. However, in this relatively small material there was no correlation between non-V $\delta$ 1V $\delta$ 2 cell proportions and MSS/MSI status, tumour differentiation, stage, location (right vs left sided), or patient age. Only when comparing men and women could we find a significantly higher proportion of non-V $\delta$ 1V $\delta$ 2 cells in the tumours from female patients (Fig. 3).

### Clonality of tumour-infiltrating $\gamma\delta$ T cells

To determine clonality, and the potential of public, shared  $\gamma\delta$  clonotypes between patients, the  $\delta$  chain CDR3 sequence was analysed.  $\delta$  chain sequencing of 10 colon tumours resulted in a total of 9,403 productive recombinations, representing individual cells, where the CDR3 sequence was reliably determined, ranging from 175 to 2,167 recombinations from individual tumours. These recombinations were

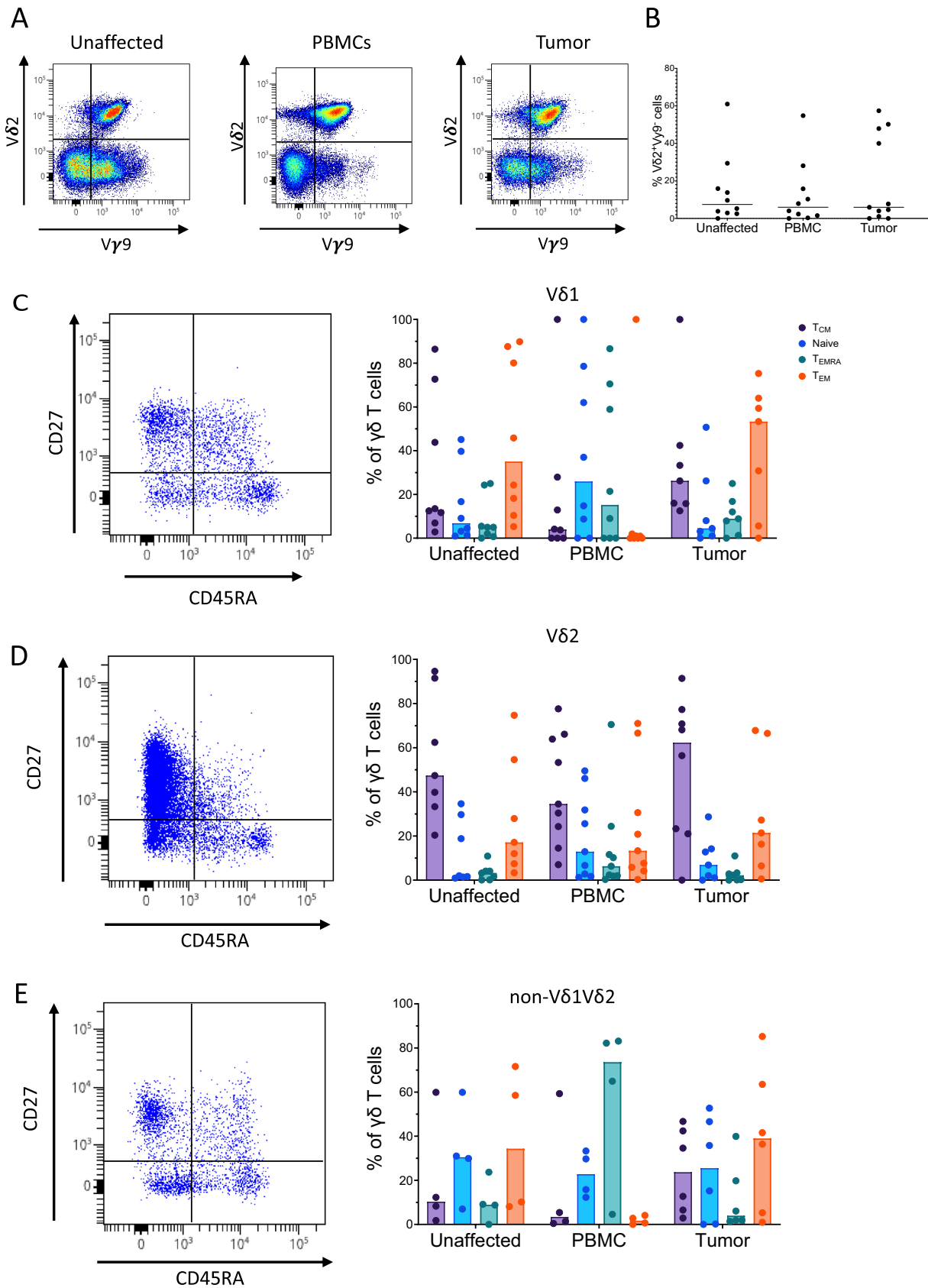


**Fig. 2** Phenotype of tumour-infiltrating  $\gamma\delta$  T cells. Single cell suspensions were isolated from tumours, corresponding unaffected colon mucosa, and blood, and analysed using flow cytometry. **A** V $\delta$ 2 and V $\gamma$ 9 staining in an unaffected tissue, blood, and tumour from a representative patient. **B** Frequencies of V $\gamma$ 9<sup>+</sup> cells among all V $\delta$ 2 cells from the different tissues. **C–E** The frequencies of central memory, naïve, terminally differentiated effector memory, and effector memory cells among the V $\delta$ 1 (**C**), V $\delta$ 2 (**D**), and non-V $\delta$ 1V $\delta$ 2 (**E**)  $\gamma\delta$  T cells are shown alongside dot plots of V $\delta$ 1, V $\delta$ 2, and non-V $\delta$ 1V $\delta$ 2 cells from tumour tissue. Symbols represent individual values and lines and bars the median. n = 4–9

distributed between 2,092 clonotypes, containing between 1 and 464 recombinations per clonotype. The distribution of clonotypes differed markedly between individual tumours (Fig. 4A). Of note, the dominating clonotypes were either V $\delta$ 1, V $\delta$ 2, or V $\delta$ 3 in different tumours. However, in all but one of the patients, V $\delta$ 3 cells made up one to five of the ten dominating clonotypes (Fig. 4A, B). Unfortunately, we did not have access to unaffected tissue and blood from these individuals and could thus not investigate to which extent these clones were present in healthy tissues. The difference in  $\gamma\delta$  T cells between individual tumours was also reflected in the Gini-Simpson diversity index, which varied between 0.49 and 0.77 in the different tumours. There was no difference in diversity between cells from MSI-L/H and MSS tumours or between different stage tumours (Fig. 4C). Furthermore, there was no overlap between the clonotypes found in any patients, further emphasizing the large inter-individual variation in  $\gamma\delta$  T cell composition between patients.

### Mass cytometry and mRNA quantification reveal diverse clusters of tumour-infiltrating $\gamma\delta$ T cells

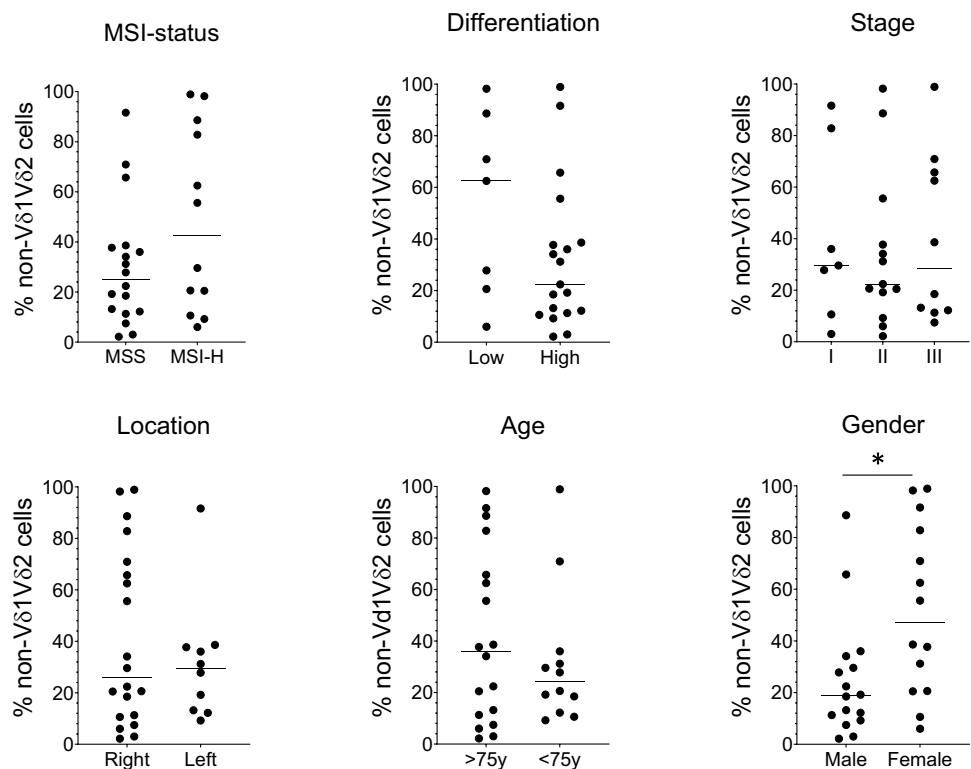
To gain additional understanding of the different subsets of  $\gamma\delta$  T cells beyond  $\delta$  chain usage, we employed a panel of antibodies focused on cytotoxicity and exhaustion markers and analysed *ex-vivo* isolated T cells using mass cytometry.  $\gamma\delta$  T cells were manually gated as live CD45<sup>+</sup>CD3<sup>+</sup>CD4<sup>-</sup>TCR  $\gamma\delta$ <sup>+</sup> cells, and unsupervised dimensional reduction of the aggregated data from all patients was performed using the UMAP algorithm, followed by clustering using the phenograph algorithm. Initially, we clustered 59,110  $\gamma\delta$  T cells from tumours, 38,275 from unaffected colon mucosa, and 204,561 from PBMC collected from 18 patients (Fig. 5A). From these analyses, it was clear that  $\gamma\delta$  T cells from blood and the colon tissue formed distinct clusters with low or no overlap (Fig. 5B). As the tumour-infiltrating lymphocytes presumably are the most relevant for anti-tumour immunity, we subsequently focused on their phenotype and effector functions. We thus performed unsupervised analysis of 59,110 tumour-infiltrating  $\gamma\delta$  T cells (Fig. 5C). Based

on the expression of the V $\delta$ 1 or V $\delta$ 2 chain, 3 distinct groups containing V $\delta$ 1, V $\delta$ 2, and non-V $\delta$ 1V $\delta$ 2 cells were observed (Fig. 5D) In the tumours, we could identify 10 clusters of V $\delta$ 1 cells, 13 clusters of V $\delta$ 2 cells, and a single cluster of non-V $\delta$ 1V $\delta$ 2 cells (cluster 15). Expression of individual markers across the UMAP projection is shown in Suppl. Fig. S4. The contribution of cells from individual tumours to a certain cluster differed. Most clusters were made up of cells from all the tumours, while some clusters (e.g. cluster 18 and 20) consisted mainly of cells from a single tumour (Suppl. Fig. S5). While expression of several markers could be found in most clusters present in the tumours, other markers varied substantially in expression. For instance, the V $\delta$ 1 cells generally had a higher expression of CD103, CD38, and the exhaustion markers TIGIT, PD-1 (CD279), and CD39 compared to the other subsets. In contrast, the V $\delta$ 2 clusters were much more diverse with expression of several markers unique to only one or two clusters (Fig. 5E). The single non-V $\delta$ 1V $\delta$ 2 cluster present in the tumours had a high expression of CD45RO and Fas (CD95), and also a higher expression than most other clusters of several proteins expressed in activated cells, such as ICOS (CD254), OX-40 (CD134), CD25, and FoxP3 (Fig. 5E).

In a separate set of four patients, the tumour-infiltrating V $\delta$ 1, V $\delta$ 2, and non-V $\delta$ 1V $\delta$ 2 cells were sorted by flow cytometry immediately after isolation, and mRNA quantified. In total, we identified 76 genes that were differentially expressed between non-V $\delta$ 1V $\delta$ 2 and V $\delta$ 1 or V $\delta$ 2 cells (Suppl. Table S4). V $\delta$ 1 cells presented a signature consistent with cytotoxic effector functions, with a high expression of *GNLY* (Granulysin), *PRF1* (Perforin), *CD244* (2B4), and *NCR1* (NKG2A) (Fig. 6A, B). A cytotoxic effector signature could also be observed when comparing the V $\delta$ 2 and the non-V $\delta$ 1V $\delta$ 2 cells. However, in addition to *PRF1*, the V $\delta$ 2 transcriptome was dominated by expression of *GRZK* and *GRZB* (granzymes K and B), the killer cell lectin-like receptors *KLRG1*, *KLRC1* (NKG2A), and *KLRB1* (CD161; Fig. 6A, B). Interestingly, the non-V $\delta$ 1V $\delta$ 2 cells had a higher expression of genes associated with inflammatory and tumour-promoting responses, such as *CXCL1* (GRO- $\alpha$ ), *CXCL2* (GRO- $\beta$ ), *IL8* (IL-8), *TGFBI* (transforming growth factor-beta induced, TGFBI), and *LGALS3* (Galectin-3), and several genes associated with antigen presentation (*HLA-DPA1*, *HLA-DQA1*, *HLA-DRB3*, and *CD74*), when compared to the other subsets (Fig. 6C).

Taken together, these analyses show that V $\delta$ 1 and V $\delta$ 2 cells express markers that are associated with cytotoxic effector functions. In contrast, the non-V $\delta$ 1V $\delta$ 2 cells appear to have a more tumour-promoting function, as they express less NK cell receptors and cytotoxic effector molecules, but

**Fig. 3** Tumour-infiltrating non-V $\delta$ 1V $\delta$ 2 cells and tumour characteristics. Single cell suspensions were isolated from tumours, and the frequencies of non-V $\delta$ 1V $\delta$ 2 cells among the  $\gamma\delta$  T cells were determined by flow cytometry and related to MSI status, tumour differentiation, stage, and location, and patient age and gender. Symbols represent individual values and lines the median. Data were analysed using two-tailed Wilcoxon test. \* $p < 0.05$ .  $n = 30$



instead markers associated with an innate inflammatory immune response and direct tumour-promoting functions.

### Cytokine production in tumour-infiltrating $\gamma\delta$ T cells

To better understand the functional capacity of the non-V $\delta$ 1V $\delta$ 2 cell subset in colon cancer patients, we analysed the production of Th1 and Th17 associated cytokines and GrB following polyclonal stimulation. These experiments revealed that IFN- $\gamma$  was highly expressed especially in V $\delta$ 2 cells from all tissues. In contrast, the non-V $\delta$ 1V $\delta$ 2 cells from the unaffected colon mucosa and the tumours only contained moderate frequencies of IFN- $\gamma$ -producing cells (Fig. 7A). TNF production was considerably lower than that of IFN- $\gamma$  and was also lower in the non-V $\delta$ 1V $\delta$ 2 subset compared to the V $\delta$ 2 subset in the cells present in both the tissue and the circulation (Fig. 7B). In contrast, IL-17A expression was only seen in non-V $\delta$ 1V $\delta$ 2 cells from some individuals, but virtually not in any of the other subsets of  $\gamma\delta$  T cells (Fig. 7C). This was similar to IL-8 expression, which was only detected in some patients and primarily in circulating non-V $\delta$ 1V $\delta$ 2 cells (Fig. 7D). GrB, on the other hand, was expressed at relatively high levels in cells from all tissues from all patients. Furthermore, there were no substantial differences in GrB production between the  $\gamma\delta$  T cell subsets from the tumours using different TCRs (Fig. 7E). Representative flow cytometry plots from one patient can be found in Suppl. Fig. S6–S8. The median fluorescence intensity of

the cells staining positive for the respective cytokines was generally similar between the  $\gamma\delta$  T cells subsets, except for GrB staining intensity which was especially high in V $\delta$ 1 and non-V $\delta$ 1 V $\delta$ 2 cells from the circulation (Suppl. Fig. S9). In general, GrB production from  $\gamma\delta$  T cells was higher than in conventional  $\alpha\beta$  T cells, while TNF and IL-17 production was lower and IFN- $\gamma$  and IL-8 production was similar to that in  $\alpha\beta$  T cells (Suppl. Fig. S10).

### Discussion

Recent studies in CRC show the presence of different subsets of tumour-infiltrating  $\gamma\delta$  T cells with specific functions, which range from tumour-promoting to tumoricidal effects [11, 26]. This is likely context dependent and is yet to be fully understood. In this study, we used several strategies to delineate different subpopulations of tumour-infiltrating  $\gamma\delta$  T cells in colon cancer patients. We show that  $\gamma\delta$  T cell infiltration into tumours was reduced in most patients, compared to the surrounding unaffected colon mucosa, and that the tumour-infiltrating  $\gamma\delta$  T cells vary considerably between patients with regard to V $\delta$  chain usage, phenotype, and functional properties.

Most research on human  $\gamma\delta$  T cells has focused on V $\delta$ 1 and V $\delta$ 2 cells, mainly due to the limited availability of antibodies to the other TCRs. However, in human tissues there is a considerable proportion of  $\gamma\delta$  T cells using other V $\delta$

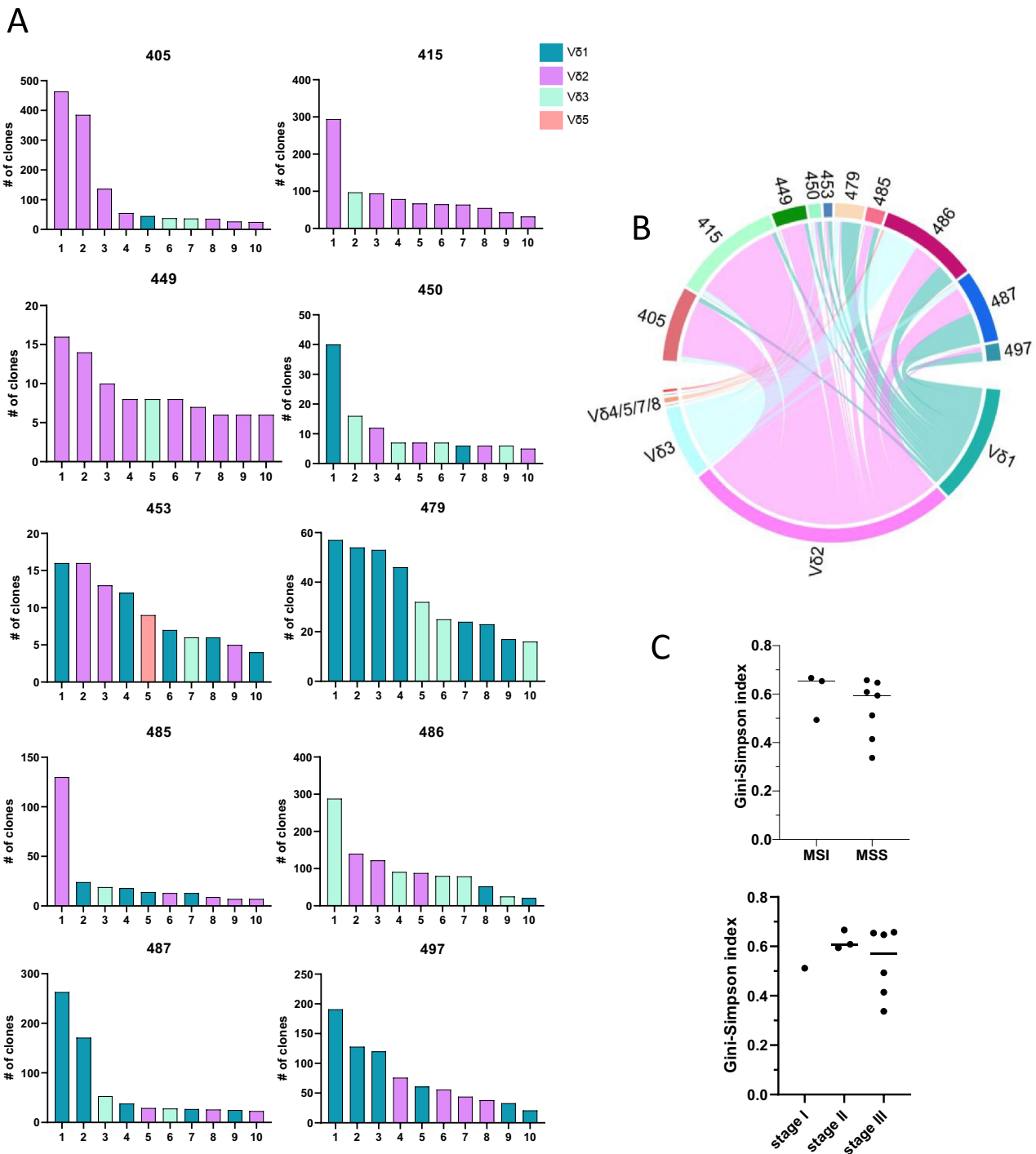


**Fig. 4** Vδ chain usage in tumour-infiltrating γδ T cells. Single cell suspensions were isolated from frozen tumour specimens and the CDR3 region analysed with ultra-sensitive sequencing using unique molecular identifiers. **A** The number of clones in the ten most frequent clonotypes from each patient. Colour coding shows the Vδ usage in the respective clonotypes. **B** Chord diagram showing the

distribution of clones using the different Vδ chains in individual patients. **C** Gini-Simpson index of diversity was calculated for each tumour and plotted as a function of microsatellite status and tumour stage. Symbols represent individual values and the line the median. n = 10

chains, both in tumours and the corresponding healthy tissue [5, 11, 26–28]. Here, we could document a similar accumulation of non-Vδ1Vδ2 cells in human colon tissues. In the

tumours, TCR sequencing showed that these cells expressed Vδ3 to a very large extent and also contributed to the most expanded clonotypes in most of the patients. The Vδ3 cells



**Fig. 5** Clustering analysis of tumour-infiltrating  $\gamma\delta$  T cells. Single cell suspensions were isolated from tumours, corresponding unaffected colon mucosa, and blood, and analysed using mass cytometry. **A**  $\gamma\delta$  T cells were first analysed using the UMAP dimensional reduction algorithm in concatenated data combined from blood, tumour, and unaffected tissue. **B** Data from **A** are shown individually for unaffected tissue, PBMCs, and tumours. **C** Tumour-infiltrating  $\gamma\delta$  T cells were analysed separately using the UMAP dimensional reduction algorithm together with the phenograph clustering algorithm. The markers indicated in **(E)** were all used to generate the clustering algorithms. **D** Expression of V $\delta$ 1 and V $\delta$ 2 overlaid on the clustered tumour-infiltrating  $\gamma\delta$  T cells. The colour scale represents staining intensity, and the scale is based on the minimum to the maximum signal in each specific marker. **E** Heatmap of marker expression in the clusters identified in tumour-infiltrating  $\gamma\delta$  T cells using the UMAP dimensional reduction and phenograph clustering algorithms. The colour scale shows the median signal intensity of the respective marker in each cluster, and the scales were generated individually for each marker and based on the minimum to the maximum signal in each specific marker.  $n=18$

in the tumours were often oligoclonal with one or a few dominating clones, and they may recognize tumour neoantigens or stress signals in the tumour cells, such as Annexin A2 [29]. The cognate ligands for V $\delta$ 3 cells also include the monomorphic MHC I-like molecules CD1d and MR1 [30, 31]. These molecules are also increased on the cell surface following endoplasmic reticulum (ER) stress and inflammatory signals [32, 33], and reactivity against such antigens may also explain some of the clonal expansion of V $\delta$ 3 cells in the tumours.

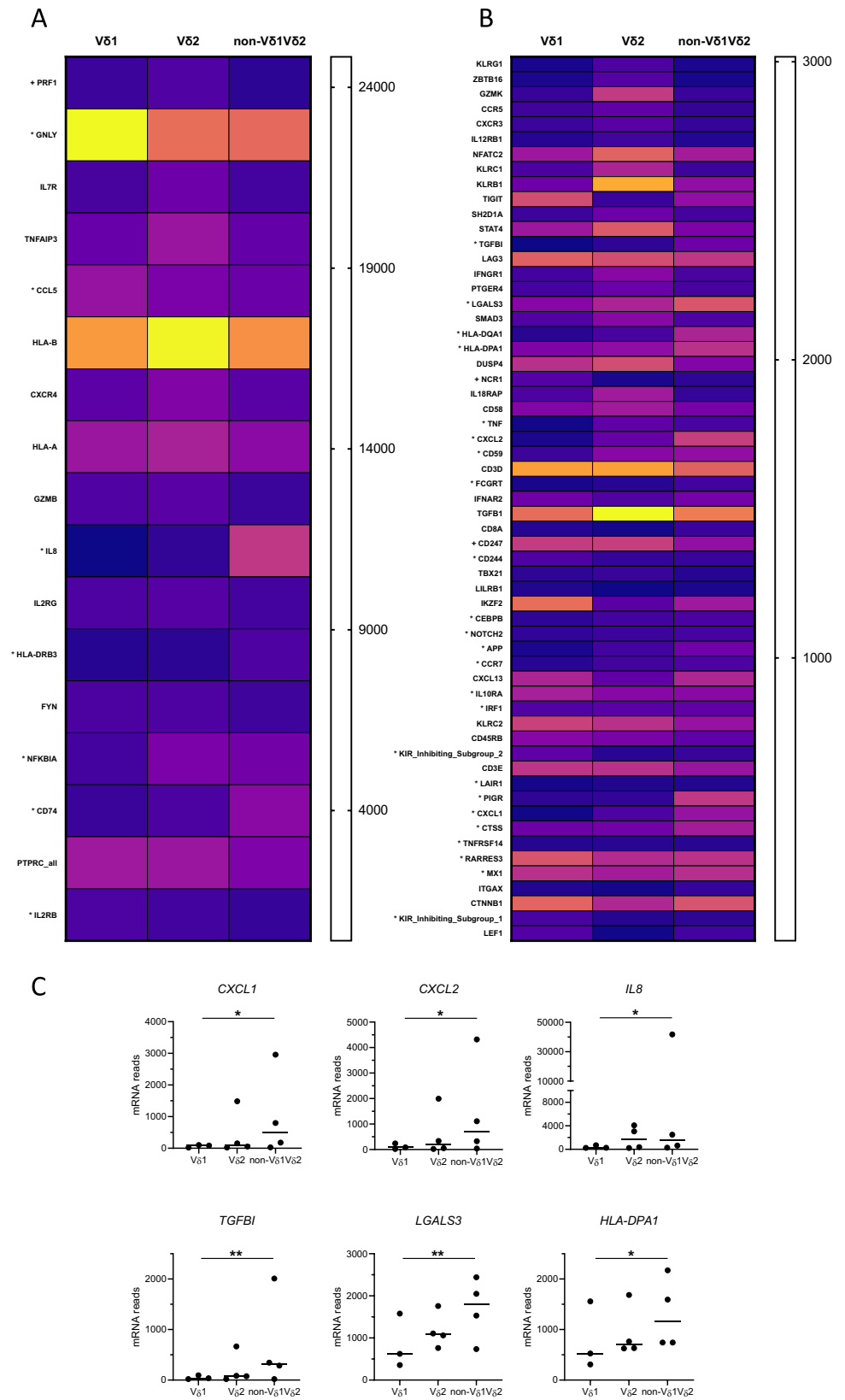
We have used CD27 and CD45RA as markers of different memory populations, even though this nomenclature was originally devised for  $\alpha\beta$  T cells. V $\delta$ 1 and non-V $\delta$ 1 V $\delta$ 2 cells from colon, both unaffected and tumour tissue, harboured a large proportion of T<sub>EM</sub>-like cells which were not present among the circulating cells. This is similar to tissue-infiltrating  $\gamma\delta$  T cells in liver tissue and non-small cell lung cancer, where similar T<sub>EM</sub>-like V $\delta$ 1 cells have been documented [34, 35]. In the V $\delta$ 1 and non-V $\delta$ 1 V $\delta$ 2 cells, the distribution between memory subsets was conserved in colon mucosa and tumours, but different in blood, while V $\delta$ 2 cells were similar with regard to memory subsets in blood and tissues. Therefore, we cannot rule out the possibility that a substantial proportion of the V $\delta$ 2 cells detected in the colon tissues may in fact originate from the microvasculature, while V $\delta$ 1 and non-V $\delta$ 1 V $\delta$ 2 cells might more likely represent tissue-resident cells, as previously documented in lung and ovarian cancer [35, 36].

Both V $\delta$ 1 and V $\delta$ 2 cells have been attributed potent anti-tumour effects, while the effect of other  $\gamma\delta$  T cells in the tumour microenvironment is more elusive [37]. V $\delta$ 1 cells possess potent cytotoxic activity towards cancer cells in vitro and a high expression of cytotoxic effector proteins, such as Granzyme B [5, 38]. Previous detailed transcriptional analyses of tumour-infiltrating  $\gamma\delta$  T cells revealed distinct

clusters based on the transcriptional profiles of V $\delta$ 1 and V $\delta$ 2 cells that exhibited similar expression of cytotoxic markers as the clusters of CD8<sup>+</sup> T cells and NK cells [28]. In our study, we identified several clusters of both V $\delta$ 1 and V $\delta$ 2 cells with both overlapping and unique features. A distinct feature of V $\delta$ 1 and V $\delta$ 2 cells from both cell surface staining and mRNA quantification was a strong cytotoxic profile comprising both NK cell receptors and cytotoxic effector molecules. Still, cytotoxic molecules and NK cell receptors were partly differentially expressed, as previously described [28, 39]. Using a mass cytometry panel, all non-V $\delta$ 1V $\delta$ 2  $\gamma\delta$  T cells formed a single and relatively small cluster. This is somewhat different to the flow cytometry results and may be explained by the less distinct signals in mass compared to flow cytometry. The non-V $\delta$ 1V $\delta$ 2 cells were characterized by a low surface expression of NK cell receptors and also appeared to be more activated, while they showed little sign of exhaustion. Non-V $\delta$ 1V $\delta$ 2 cells also had higher mRNA expression of neutrophil-recruiting chemokines, a tumour-promoting factor [7]. Furthermore, one of the genes we identified as more highly expressed by non-V $\delta$ 1V $\delta$ 2 cells was *TGFBI*. *TGFBI* has been implicated in tumour progression, and elevated levels have been associated with a poor clinical outcome, as it promotes angiogenesis and tumour cell migration, not least in CRC [40], and also reduces T cell activation [41, 42]. The expression of Galectin-3 in non-V $\delta$ 1V $\delta$ 2 cells is also interesting, as recent studies link Galectin-3 production to a poor patient outcome in CRC, increased metastatic potential, and to a  $\gamma\delta$ 17 phenotype, both in healthy tissues and tumours [43, 44]. A cluster of expanded  $\gamma\delta$  T cells with high expression of Galectin-3 and other IL-17 associated genes was also recently found in human CRC tumours using single-cell RNA sequencing [26].

Functional analyses of the non-V $\delta$ 1V $\delta$ 2 cells revealed that they had a much lower expression of IFN- $\gamma$  and TNF than V $\delta$ 2 cells, suggesting a lower capacity to support anti-tumour immunity. Additionally, non-V $\delta$ 1V $\delta$ 2 cells were the main source of IL-17A among  $\gamma\delta$  T cells, even though the production was limited compared to other cytokines. This is consistent with a study by Harman et al. [11], who also found IL-17-producing  $\gamma\delta$  T cells among V $\delta$ 3 cells. The restriction of IL-17 to non-V $\delta$ 1V $\delta$ 2 cells is also in line with murine studies, where distinct  $\gamma\delta$  T cell subsets provide IL-17 in the tumour microenvironment [26, 45]. Generally, intratumoural IL-17 production has been associated with a poor prognosis [8, 12], but the source of intratumoural IL-17 is not yet fully resolved [27]. Based on our current results and previous literature, it is likely that a major part of IL-17 produced in the tumour microenvironment is provided by CD4<sup>+</sup> Th17 cells, rather than  $\gamma\delta$ 17 cells [35, 46]. Likewise, TNF production from  $\gamma\delta$  T cells may not be crucial for the overall cytokine balance in

**Fig. 6** mRNA expression in tumour-infiltrating  $\gamma\delta$  T cell subsets. Single cell suspensions were isolated from tumours and V $\delta$ 1, V $\delta$ 2, and non-V $\delta$ 1V $\delta$ 2 cells were sorted by flow cytometry and analysed using multiplex mRNA quantification. To facilitate interpretation of the data, the heatmap of differentially expressed genes has been divided into mRNAs with a high (A) and low (B) expression, respectively. Genes are presented in order of the highest to the lowest significance values of the difference between non-V $\delta$ 1V $\delta$ 2 cells and the other subsets within the two panels. The intensity scales indicate the normalized counts of mRNAs per cell. Genes marked with \* indicate significant differences between non-V $\delta$ 1V $\delta$ 2 and V $\delta$ 1 cells, while no marking indicates significant differences between non-V $\delta$ 1V $\delta$ 2 and V $\delta$ 2 cells. C mRNA counts in cell subsets from individual tumours are shown for *CXCL1*, *CXCL2*, *IL8*, *TGFBI*, *LGALS3*, and *HLA-DPA1*. Data were analysed using two-tailed Friedman test without adjustment for multiple comparisons. \* $p < 0.05$ , \*\* $p < 0.01$ . n = 4



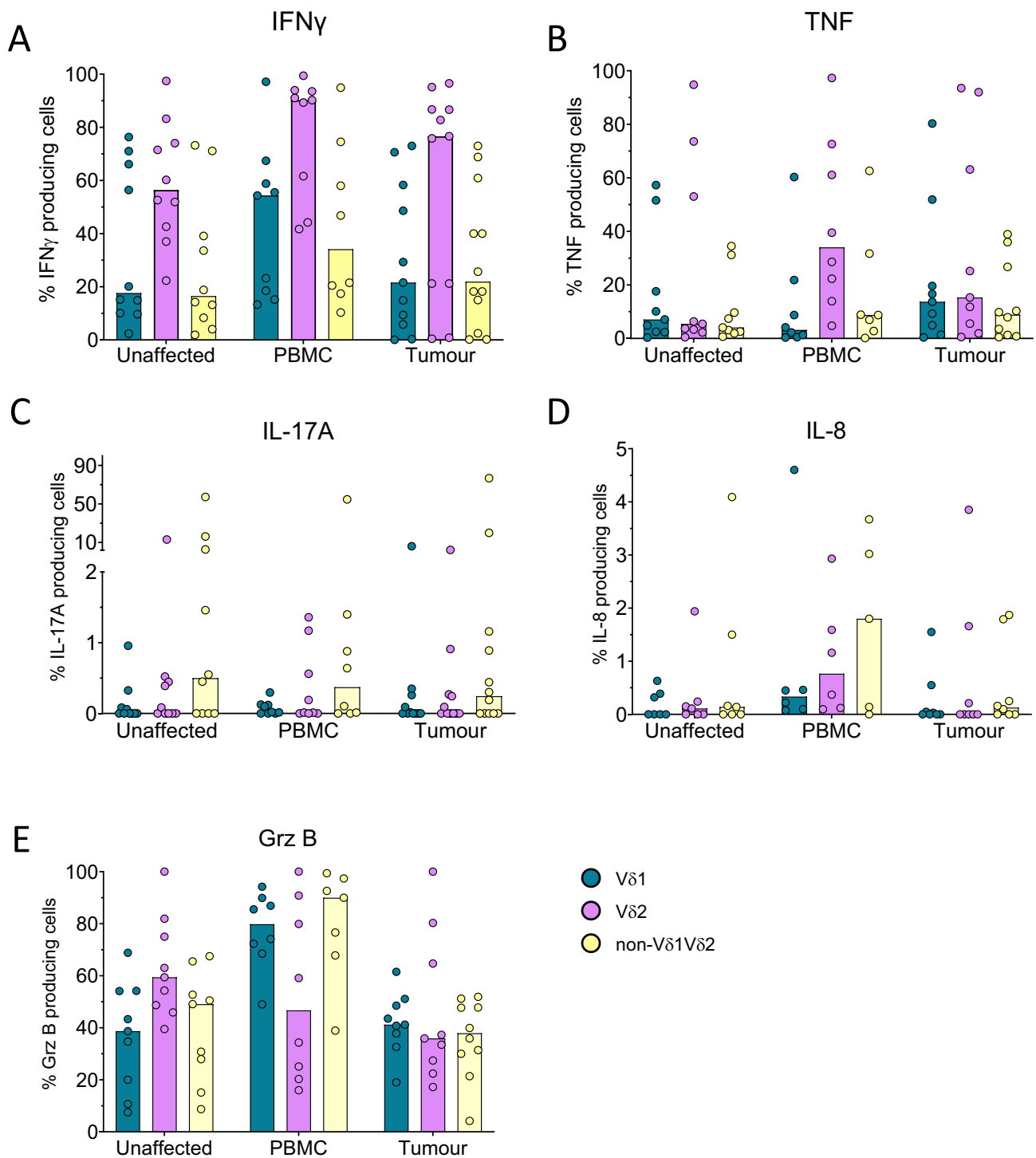


**Fig. 7** Cytokines and effector proteins in tumour-infiltrating  $\gamma\delta$  T cells. Single cell suspensions were isolated from tumours, corresponding unaffected colon mucosa, and blood, and stimulated with PMA and Ionomycin. V $\delta$ 1, V $\delta$ 2, and non-V $\delta$ 1V $\delta$ 2 cells were ana-

lysed for the expression of IFN- $\gamma$  (**A**), TNF (**B**), IL-17A (**C**), IL-8 (**D**), and Granzyme B (**E**) by flow cytometry. Symbols represent individual values and the bars the median. n=5–12

colon tumours, while  $\gamma\delta$  T cells produce IFN- $\gamma$  to an extent comparable to or higher than conventional  $\alpha\beta$  T cells.

This is a single-centre study with a well-defined patient cohort. However, one limitation of the study is the relatively small number of patients included, and the varying number

of patients used for different analyses. The latter was caused by several samples containing quite few  $\gamma\delta$  T cells, and we thus had to prioritize between assays. With a larger cohort, we might have been able to detect correlations between  $\gamma\delta$  T cell subsets or functions and patient outcome.

In summary, this study demonstrates a large variation in  $\gamma\delta$  T cell composition between individual tumours with regard to phenotypic markers, functional potential, and TCR usage. Recent studies clearly demonstrate both antitumour and tumour-promoting functions of tumour-infiltrating  $\gamma\delta$  T cell subsets, which were distinguished based on TCR usage [11, 26]. Our results show substantial infiltration of non-V $\delta$ 1V $\delta$ 2 cells, primarily using V $\delta$ 3, in colon tumours and based on their low expression of cytotoxic molecules combined with higher expression of some tumour-promoting mediators, we suggest that they contribute mainly to a tumour-promoting immune response.

**Supplementary Information** The online version contains supplementary material available at <https://doi.org/10.1007/s00262-024-03758-7>.

**Acknowledgements** We would like to thank all patients for their participation in this study and Angelica Wingård and Zunash Malik at the Surgical Oncology Laboratory at Sahlgrenska University Hospital for their valuable assistance with collection of clinical samples. This work was supported by the Swedish Research Council (2021-01361 and 2021-01008), the Swedish Cancer Foundation (21-1646 and 22-2080), grants from the Swedish state under the agreement between the Swedish government and the county councils, the ALF agreement (144381 and 965065), Region Västra Götaland, the Sjöberg Foundation, and Assar Gabrielsson Foundation.

**Author contribution** MQJ conceptualized the study; WR, LS, TR, FTK, TÖ, PS, and SH helped in methodology; WR, LS, TR, FTK, TÖ, and MQJ contributed to formal analysis and investigation; AS, EBL, and MQJ were involved in funding acquisition; AC, AS, EBL, and MQJ supervised the study; YW, AC, AS, and EBL helped in resources; WR and MQJ were involved in writing—original draft preparation; all authors helped in writing—review and editing.

**Funding** Open access funding provided by University of Gothenburg. This work was supported by the Swedish Research Council (55X-13428 and 2021-01008), the Swedish Cancer Foundation (130593 and 22-2080), grants from the Swedish state under the agreement between the Swedish government and the county councils, the ALF agreement (144381 and 965065), Region Västra Götaland, the Sjöberg Foundation, and Assar Gabrielsson Foundation.

**Data availability** TCR sequencing raw data in fastq format have been deposited to the NCBI short read archive (SRA; <https://www.ncbi.nlm.nih.gov/sra>) with accession number PRJNA1107040. Normalized Nanostring data have been deposited to Gene Expression Omnibus (GEO; <https://www.ncbi.nlm.nih.gov/geo/>) with accession number GSE266504.

## Declarations

**Conflict of interest** AS declares stock ownership and is a board member in Tulebovaasta, Iscaff Pharma, and SiMSen Diagnostics. AS is co-inventor of the SiMSen-Seq technology that is patent protected (US

Serial No.:15/552,618). MQJ has received consultancy fees from Biomunex Pharmaceuticals.

**Ethical approval** This study was performed according to the Declaration of Helsinki and approved by the Regional Board of Ethics in Medical Research in west Sweden (249–15, approved 06/03/2015).

**Consent to participate** All patients gave a written informed consent before participation in the study.

**Open Access** This article is licensed under a Creative Commons Attribution 4.0 International License, which permits use, sharing, adaptation, distribution and reproduction in any medium or format, as long as you give appropriate credit to the original author(s) and the source, provide a link to the Creative Commons licence, and indicate if changes were made. The images or other third party material in this article are included in the article's Creative Commons licence, unless indicated otherwise in a credit line to the material. If material is not included in the article's Creative Commons licence and your intended use is not permitted by statutory regulation or exceeds the permitted use, you will need to obtain permission directly from the copyright holder. To view a copy of this licence, visit <http://creativecommons.org/licenses/by/4.0/>.

## References

1. Kazen AR, Adams EJ (2011) Evolution of the V, D, and J gene segments used in the primate gammadelta T-cell receptor reveals a dichotomy of conservation and diversity. *Proc Natl Acad Sci U S A* 108:E332–E340. <https://doi.org/10.1073/pnas.1105105108>
2. Papadopoulou M, Sanchez Sanchez G, Vermijlen D (2020) Innate and adaptive gammadelta T cells: How, when, and why. *Immunol Rev* 298:99–116. <https://doi.org/10.1111/imr.12926>
3. Clark BL, Thomas PG (2020) A Cell for the ages: human gammadelta T cells across the lifespan. *Int J Mol Sci*. <https://doi.org/10.3390/ijms21238903>
4. Simoes AE, Di Lorenzo B, Silva-Santos B (2018) Molecular Determinants of Target Cell Recognition by Human gammadelta T Cells. *Front Immunol* 9:929. <https://doi.org/10.3389/fimmu.2018.00929>
5. Mikulak J, Oriolo F, Bruni E et al (2019) NKp46-expressing human gut-resident intraepithelial Vdelta1 T cell subpopulation exhibits high antitumor activity against colorectal cancer. *JCI Insight*. <https://doi.org/10.1172/jci.insight.125884>
6. Park JH, Lee HK (2021) Function of gammadelta T cells in tumor immunology and their application to cancer therapy. *Exp Mol Med* 53:318–327. <https://doi.org/10.1038/s12276-021-00576-0>
7. Gentles AJ, Newman AM, Liu CL et al (2015) The prognostic landscape of genes and infiltrating immune cells across human cancers. *Nat Med* 21:938–945. <https://doi.org/10.1038/nm.3909>
8. Meraviglia S, Lo Presti E, Tosolini M et al (2017) Distinctive features of tumor-infiltrating gammadelta T lymphocytes in human colorectal cancer. *Oncoimmunology* 6:e1347742. <https://doi.org/10.1080/2162402X.2017.1347742>
9. Thorsson V, Gibbs DL, Brown SD et al (2018) The Immune Landscape of Cancer. *Immunity* 48(812–30):e14. <https://doi.org/10.1016/j.immuni.2018.03.023>
10. Yu L, Wang Z, Hu Y, Wang Y, Lu N, Zhang C (2023) Tumor-infiltrating gamma delta T-cells reveal exhausted subsets with remarkable heterogeneity in colorectal cancer. *Int J Cancer* 153:1684–1697. <https://doi.org/10.1002/ijc.34669>
11. Harmon C, Zaborowski A, Moore H et al (2023) gammadelta T cell dichotomy with opposing cytotoxic and wound healing

- functions in human solid tumors. *Nat Cancer* 4:1122–1137. <https://doi.org/10.1038/s43018-023-00589-w>
12. Tosolini M, Kirilovsky A, Mlecnik B et al (2011) Clinical impact of different classes of infiltrating T cytotoxic and helper cells (Th1, th2, treg, th17) in patients with colorectal cancer. *Cancer Res* 71:1263–1271. <https://doi.org/10.1158/0008-5472.CAN-10-2907>
  13. Bindea G, Mlecnik B, Tosolini M et al (2013) Spatiotemporal dynamics of intratumoral immune cells reveal the immune landscape in human cancer. *Immunity* 39:782–795. <https://doi.org/10.1016/j.immuni.2013.10.003>
  14. Ma S, Cheng Q, Cai Y et al (2014) IL-17A produced by gammadelta T cells promotes tumor growth in hepatocellular carcinoma. *Cancer Res* 74:1969–1982. <https://doi.org/10.1158/0008-5472.CAN-13-2534>
  15. Sutton CE, Lalor SJ, Sweeney CM, Brereton CF, Lavelle EC, Mills KH (2009) Interleukin-1 and IL-23 induce innate IL-17 production from gammadelta T cells, amplifying Th17 responses and autoimmunity. *Immunity* 31:331–341. <https://doi.org/10.1016/j.immuni.2009.08.001>
  16. Wu D, Wu P, Qiu F, Wei Q, Huang J (2017) Human gammadeltaT-cell subsets and their involvement in tumor immunity. *Cell Mol Immunol* 14:245–253. <https://doi.org/10.1038/cmi.2016.55>
  17. Sundstrom P, Szeponik L, Ahlmanner F, Sundquist M, Wong JSB, Lindskog EB, Gustafsson B, Quiding-Jarbrink M (2019) Tumor-infiltrating mucosal-associated invariant T (MAIT) cells retain expression of cytotoxic effector molecules. *Oncotarget* 10:2810–2823. <https://doi.org/10.18632/oncotarget.26866>
  18. Lundgren A, Stromberg E, Sjolting A et al (2005) Mucosal FOXP3-expressing CD4+ CD25high regulatory T cells in Helicobacter pylori-infected patients. *Infect Immun* 73:523–531. <https://doi.org/10.1128/IAI.73.1.523-531.2005>
  19. Liang F, Rezapour A, Falk P, Angenete E, Yrlid U (2021) Cryopreservation of whole tumor biopsies from rectal cancer patients enable phenotypic and in vitro functional evaluation of tumor-infiltrating T cells. *Cancers (Basel)*. <https://doi.org/10.3390/cancers13102428>
  20. Johansson G, Kaltak M, Rimniceanu C et al (2020) Ultrasensitive DNA Immune Repertoire Sequencing Using Unique Molecular Identifiers. *Clin Chem* 66:1228–1237. <https://doi.org/10.1093/clinchem/hvaa159>
  21. Shugay M, Britanova OV, Merzlyak EM et al (2014) Towards error-free profiling of immune repertoires. *Nat Methods* 11:653–655. <https://doi.org/10.1038/nmeth.2960>
  22. Szeponik L, Ahlmanner F, Sundstrom P, Rodin W, Gustavsson B, Bexé Lindskog E, Wettergren Y, Quiding-Jarbrink M (2021) Intratumoral regulatory T cells from colon cancer patients comprise several activated effector populations. *BMC Immunol* 22:58. <https://doi.org/10.1186/s12865-021-00449-1>
  23. Mei HE, Leipold MD, Schulz AR, Chester C, Maecker HT (2015) Barcoding of live human peripheral blood mononuclear cells for multiplexed mass cytometry. *J Immunol* 194:2022–2031. <https://doi.org/10.4049/jimmunol.1402661>
  24. Davey MS, Willcox CR, Hunter S et al (2018) The human Vdelta2(+) T-cell compartment comprises distinct innate-like Vgamma9(+) and adaptive Vgamma9(-) subsets. *Nat Commun* 9:1760. <https://doi.org/10.1038/s41467-018-04076-0>
  25. Odaira K, Kimura SN, Fujieda N, Kobayashi Y, Kambara K, Takahashi T, Izumi T, Matsushita H, Kakimi K (2016) CD27(-) CD45(+) gammadelta T cells can be divided into two populations, CD27(-)CD45(int) and CD27(-)CD45(hi) with little proliferation potential. *Biochem Biophys Res Commun* 478:1298–1303. <https://doi.org/10.1016/j.bbrc.2016.08.115>
  26. Reis BS, Darcy PW, Khan IZ et al (2022) TCR-Vgammadelta usage distinguishes protumor from antitumor intestinal gammadelta T cell subsets. *Science* 377:276–284. <https://doi.org/10.1126/science.abj8695>
  27. Wu P, Wu D, Ni C et al (2014) gammadeltaT17 cells promote the accumulation and expansion of myeloid-derived suppressor cells in human colorectal cancer. *Immunity* 40:785–800. <https://doi.org/10.1016/j.immuni.2014.03.013>
  28. Pizzolato G, Kaminski H, Tosolini M et al (2019) Single-cell RNA sequencing unveils the shared and the distinct cytotoxic hallmarks of human TCRVdelta1 and TCRVdelta2 gammadelta T lymphocytes. *Proc Natl Acad Sci U S A* 116:11906–11915. <https://doi.org/10.1073/pnas.1818488116>
  29. Marlin R, Pappalardo A, Kaminski H et al (2017) Sensing of cell stress by human gammadelta TCR-dependent recognition of annexin A2. *Proc Natl Acad Sci U S A* 114:3163–3168. <https://doi.org/10.1073/pnas.1621052114>
  30. Mangan BA, Dunne MR, O'Reilly VP, Dunne PJ, Exley MA, O'Shea D, Scotet E, Hogan AE, Doherty DG (2013) Cutting edge: CD1d restriction and Th1/Th2/Th17 cytokine secretion by human Vdelta3 T cells. *J Immunol* 191:30–34. <https://doi.org/10.4049/jimmunol.1300121>
  31. Rice MT, von Borstel A, Chevoir P et al (2021) Recognition of the antigen-presenting molecule MR1 by a Vdelta3(+) gammadelta T cell receptor. *Proc Natl Acad Sci U S A*. <https://doi.org/10.1073/pnas.2110288118>
  32. Bedard M, Shrestha D, Priestman DA et al (2019) Sterile activation of invariant natural killer T cells by ER-stressed antigen-presenting cells. *Proc Natl Acad Sci U S A* 116:23671–23681. <https://doi.org/10.1073/pnas.1910097116>
  33. Ussher JE, van Wilgenburg B, Hannaway RF et al (2016) TLR signaling in human antigen-presenting cells regulates MR1-dependent activation of MAIT cells. *Eur J Immunol* 46:1600–1614. <https://doi.org/10.1002/eji.201545969>
  34. Hunter S, Willcox CR, Davey MS, Kasatskaya SA, Jeffery HC, Chudakov DM, Oo YH, Willcox BE (2018) Human liver infiltrating gammadelta T cells are composed of clonally expanded circulating and tissue-resident populations. *J Hepatol* 69:654–665. <https://doi.org/10.1016/j.jhep.2018.05.007>
  35. Wu Y, Biswas D, Usaite I et al (2022) A local human Vdelta1 T cell population is associated with survival in nonsmall-cell lung cancer. *Nat Cancer* 3:696–709. <https://doi.org/10.1038/s43018-022-00376-z>
  36. Foord E, Arruda LCM, Gaballa A, Klynning C, Uhlin M (2021) Characterization of ascites- and tumor-infiltrating gammadelta T cells reveals distinct repertoires and a beneficial role in ovarian cancer. *Sci Transl Med*. <https://doi.org/10.1126/scitranslmed.abb0192>
  37. Willcox BE, Willcox CR (2019) gammadelta TCR ligands: the quest to solve a 500-million-year-old mystery. *Nat Immunol* 20:121–128. <https://doi.org/10.1038/s41590-018-0304-y>
  38. Wu D, Wu P, Wu X et al (2015) Ex vivo expanded human circulating Vdelta1 gammadeltaT cells exhibit favorable therapeutic potential for colon cancer. *Oncoimmunology* 4:e992749. <https://doi.org/10.4161/2162402X.2014.992749>
  39. Cazzetta V, Bruni E, Terzoli S et al (2021) NKG2A expression identifies a subset of human Vdelta2 T cells exerting the highest antitumor effector functions. *Cell Rep* 37:109871. <https://doi.org/10.1016/j.celrep.2021.109871>
  40. Corona A, Blobe GC (2021) The role of the extracellular matrix protein TGFBI in cancer. *Cell Signal* 84:110028. <https://doi.org/10.1016/j.cellsig.2021.110028>
  41. Patry M, Teinturier R, Goehrig D, Zetu C, Ripoche D, Kim IS, Bertolino P, Hennino A (2015) Betaig-h3 represses T-cell activation in type 1 diabetes. *Diabetes* 64:4212–4219. <https://doi.org/10.2337/db15-0638>
  42. Lecker LSM, Berlato C, Maniati E et al (2021) TGFBI production by macrophages contributes to an immunosuppressive

- microenvironment in ovarian cancer. *Cancer Res* 81:5706–5719. <https://doi.org/10.1158/0008-5472.CAN-21-0536>
43. Wu KL, Huang EY, Yeh WL, Hsiao CC, Kuo CM (2017) Synergistic interaction between galectin-3 and carcinoembryonic antigen promotes colorectal cancer metastasis. *Oncotarget* 8:61935–61943. <https://doi.org/10.18632/oncotarget.18721>
44. Wang C, Zhou X, Ma L et al (2019) Galectin-3 may serve as a marker for poor prognosis in colorectal cancer: a meta-analysis. *Pathol Res Pract* 215:152612. <https://doi.org/10.1016/j.prp.2019.152612>
45. Szeponik L, Akeus P, Rodin W, Raghavan S, Quiding-Jarbrink M (2020) Regulatory T cells specifically suppress conventional CD8alphabeta T cells in intestinal tumors of APC(Min/+) mice. *Cancer Immunol Immunother* 69:1279–1292. <https://doi.org/10.1007/s00262-020-02540-9>
46. Amicarella F, Muraro MG, Hirt C et al (2017) Dual role of tumour-infiltrating T helper 17 cells in human colorectal cancer. *Gut* 66:692–704. <https://doi.org/10.1136/gutjnl-2015-310016>

**Publisher's Note** Springer Nature remains neutral with regard to jurisdictional claims in published maps and institutional affiliations.